AAV-mediated transduction of songbird retina

Pranav Kumar Seth[1,2]*[†], Dominik Heyers[1,3†], Baladev Satish[1†],
Ezequiel Mendoza[4], Katrin Haase[1], Lisa Borowsky[1],
Isabelle Musielak[1], Karl-Wilhelm Koch[3,5], Regina Feederle[6],
Constance Scharff[4], Karin Dedek[1,3] and Henrik Mouritsen[1,3]*

[1]Neurosensorics Group/Animal Navigation, Institute of Biology and Environmental Sciences, Carl on Ossietzky University of Oldenburg, Oldenburg, Germany, [2]Sussex Neuroscience, School of Life Sciences, University of Sussex, Brighton, United Kingdom, [3]Research Centre for Neurosensory Science, Carl von Ossietzky University of Oldenburg, Oldenburg, Germany, [4]Institut für Biologie, Freie Universität Berlin, Berlin, Germany, [5]Department of Neuroscience, Biochemistry Group, University of Oldenburg, Oldenburg, Germany, [6]Monoclonal Antibody Core Facility, Helmholtz Zentrum München, German Research Center for Environmental Health, Neuherberg, Germany

Introduction: Genetic manipulation of murine retinal tissue through ocular administration of adeno-associated viruses (AAVs) has become a standard technique to investigate a multitude of mechanisms underlying retinal physiology. Resultantly, developments of recombinant viral vectors with improved transduction efficiency and further methodological improvements have mostly focused on murine tissue, whereas AAVs successfully targeting avian retinae have remained scarce.

Methodology: Using a custom-designed injection setup, we identified a viral serotype with the capability to successfully induce widespread transduction of the bird retina.

Results: Intravitreal administration of an AAV type 2/9 encoding for enhanced green fluorescent protein (EGFP) in night-migratory European robins (*Erithacus rubecula*) resulted in transduction coverages of up to 60% within retinal tissue. Subsequent immunohistochemical analyses revealed that the AAV2/9-EGFP serotype almost exclusively targeted photoreceptors: rods, various single cones (UV, blue, green, and red cones), and both (accessory and principal) members of double cones.

Discussion: The consistently high and photoreceptor-specific transduction efficiency makes the AAV2/9 serotype a powerful tool for carrying out genetic manipulations in avian retinal photoreceptors, thus opening a wealth of opportunities to investigate physiological aspects underlying retinal processing in birds, such as physiological recordings and/or post-transductional behavioural readouts for future vision-related research.

KEYWORDS

AAV, avian retina, photoreceptors, intravitreal injection, European robin, opsin

Introduction

Adeno-associated virus (AAV) vectors are small, single-stranded DNA viruses displaying high transduction efficiency and tropism towards a wide range of host cells (Bennett et al., 1994; Jomary et al., 1994; Li et al., 1994). Their limited capability to induce immune responses has turned them into viable gene therapy tools (Atchison et al., 1965; Balakrishnan and Jayandharan; Ronzitti et al., 2020) for the investigation and treatment of retinal disorders (Buch et al., 2008; Stieger et al., 2011; Ong et al., 2019), such as, e.g., retinal degeneration and/or photoreceptor dystrophies (Ali et al., 2000; Schlichtenbrede et al., 2003; Isiegas et al., 2016; Ziccardi et al., 2019; Bacci et al., 2022).

Over the last 2 decades, mice have turned into the standard model system for retinal viral transduction experiments. Consequently, the continuously ongoing development of recombinant viral vectors with improved transduction efficiency has mostly targeted the murine visual system. In contrast, avian tissue appears to be particularly resistant to transduction using commonly available viral tools (Ahmadiantehrani and London, 2017). Resultantly, only few recombinant viral vector types have proven capable of transducing retinal tissue in birds (Scott and Lois, 2005; Harpavat and Cepko, 2006; Williams et al., 2006; Verrier et al., 2011; Vergara and Canto-Soler, 2012; Waldner et al., 2019).

Moreover, anatomical characteristics specific to birds appear to be disadvantageous to common ocular injection routes, further impeding successful transductions: the subretinal injection method, which targets the space between the photoreceptors and the retinal pigment epithelium (RPE) (Mühlfriedel et al., 2013; Park et al., 2015; Yiu et al., 2020), causes temporary focal detachment of the retina at the injection site (Cebulla et al., 2012; Waldner et al., 2019), leading to the formation of a "suspension bubble". The subretinal space between the photoreceptors and the retinal pigment epithelium in birds is considerably smaller than in mice, thus, in addition to causing potential harm to retinal tissue within the bubble, it restricts the transduction in bird retinae to the near vicinity of the "suspension bubble" (Waldner et al., 2019).

Similarly, the suprachoroidal injection route, where the space between the sclera and the choroid is targeted for viral injections (Kansara et al., 2020; Yiu et al., 2020), is methodologically challenging in birds, since the vast majority of the avian eye remains hidden in the eye socket with only parts of the sclera being visible. This leaves the intravitreal injection route as the most feasible injection method in birds, where the viral suspension is directly injected into the vitreous chamber of the eye (Giove et al., 2010). This, however, has mainly resulted in low transduction efficiency in avian retinae with the currently available genetic tools (Waldner et al., 2019).

It is surprising that in the continuous development of new genetic tools and methodological improvements for retinal research in birds has been largely neglected over the last years. In particular because birds appear to be exceptionally well suited as model systems for vision-based research: (1) avian eyes occupy a major proportion of the head (Burton, 2008); (2) related visual brain parts occupy up to 50% of the total cranial capacity in certain bird species (Waldvogel, 1990; reviewed in Seifert et al., 2020); (3) the number of retinofugal fibers in birds outclasses that of man by a factor of 2.5 (Güntürkün et al., 1993); (4) several physiological aspects of avian vision, e.g., acuity, luminance detection and/or color discrimination easily surpass that of most mammals (Jones et al., 2007; Niu et al., 2022); (5) in contrast to the rod-dominated mouse retina (Jeon et al., 1998), many avian retinae contain foveae, i.e., areas of high cone photoreceptor density, also found in humans and other primates (Haverkamp et al., 2021). Here, we used the long-distance night-migratory European robin as a study species because its retina contains a light-dependent magnetic compass (Chetverikova et al., 2022; Günther et al., 2018; Wiltschko et al., 1993; Xu et al., 2021; Zapka et al., 2009). Moreover, its retina has recently been morphologically characterized using electron microscopy (Günther et al., 2024; 2025) and immunohistochemistry (Günther et al., 2018; Chetverikova et al., 2022; Balaji et al., 2023). These findings provide a good foundation for electrophysiological studies, which are currently rare (but see Rotov et al., 2022). Finding AAV serotypes that work in the European robin will therefore be a step forward in both the study of magnetoreception and the functional analysis of avian retinal circuits.

Materials and methods

AAV production

The generation of the plasmid was performed as described in Balaji et al. (2023). We used an AAV 2/9 serotype carrying a strong ubiquitous CAG/CAAG promoter and the enhanced green fluorescent protein (EGFP) as the fluorescent reporter. Its titer (CAG: 3.97×10^{12} VG/mL; (Balaji et al., 2023); CAAG: 1.77×10^{12} VG/mL) was quantified via genomic qPCR by the Viral Core Facility of Charité–Universitätsmedizin Berlin, Germany.

Custom-designed ocular injection apparatus

For carrying out the intravitreal injections, we used a custom-designed ocular injection apparatus, consisting of a placement slab, an angular injection unit and attached gas anesthesia delivery extensions (Figure 1A). The apparatus has been designed and constructed to meet the requirements of intravitreal injections in small passerines. The device was made with Poly Vinyl Chloride (PVC) and covered with Perbunan® which prevents unwanted loss of heat from the bird. The placement slab at the bottom was designed to provide stability to the above angular injection unit as well as resistance against sudden movements during the ocular injections (Figure 1C). The angular injection unit contained two beak holders placed on opposite sides to immobilize the bird on either side and to access both eyes easily during the injections.

The isoflurane gas used as an anaesthetic was provided to the birds with the help of a tube connecting the anesthesia device to an inlet in the beak holder. The outlet of the beak holder was connected with a suction pipe to remove excess anesthetic gas. Circular knobs attached to the beak holders enabled a movement along the antero-posterior axis to assist fixation of the bird's head. A PVC block on either side was placed horizontally next to the beak holders to position the bird's body on its side in a natural resting position while being anesthetized. The four corners of the ground

FIGURE 1
Custom-made ocular injection apparatus for intravitreal injections in birds. **(A)** Scheme of the angular injection apparatus, with the two beak holders attached to the PVC plate, and the inlet/outlet tubes attached to the beak holder. **(B)** Side view of the angular injection plate, depicting the beak holders, the inlet/outlet tubes and the metal screws for angular adjustment. **(C)** Front view of the angular injection plate, placed on top of the lower placement slab. **(D)** Schematic depiction of the placement of the experimental bird in the injection apparatus. Note the second beak holder in D can be used to inject the contralateral eye of the bird if need arises.
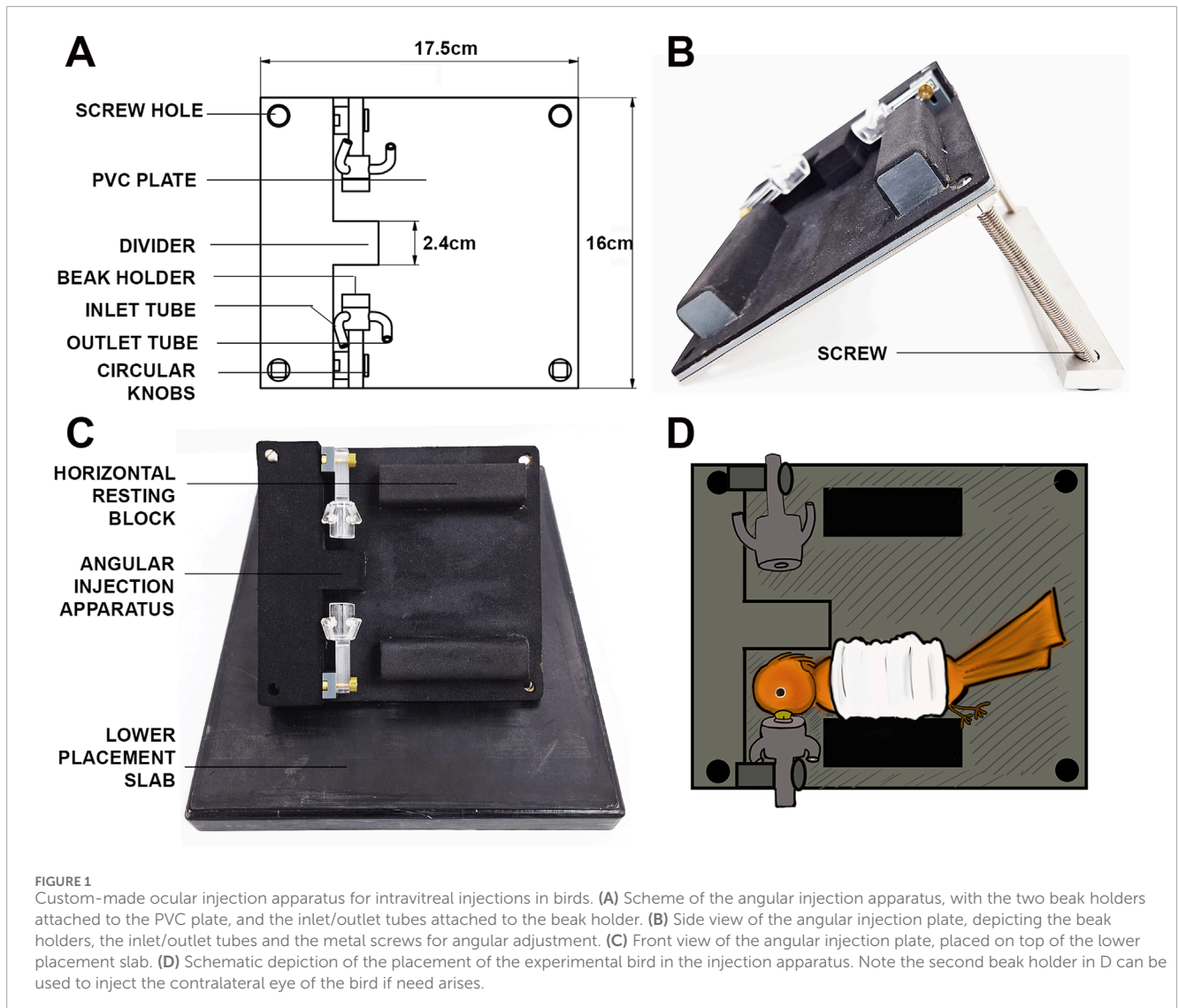
plate had screw holes to enable the adjustment of the angle of the injection unit to the ground, using two long screws at a time. In our case, an angle of approximately 30° between the angular injection unit and the lower placement slab proved optimal for intravitreal injections (Figure 1B).

Intravitreal injection protocol

Before each surgery, a single adult European robin was food-deprived for 2 h and fully anesthetized using Isoflurane CP® gas anesthesia (1 mL/mL; cp-pharma, Burgdorf, Germany) dissolved in oxygen; (2%–3% volume at initial stages of anesthesia, ~1.5% volume throughout the surgery) directed through the beak holder. Meloxicam (Metacam®, Boehringer Ingelheim, Ingelheim, Germany; 0.2 mL/kg body weight dissolved in 0.9% NaCl) was administered intramuscularly for post-surgical analgesia. The bird was wrapped with a bandage cloth to prevent wing movement and placed in the custom-designed injection apparatus (Figure 1D). The anaesthetized bird´s head was carefully fixed by inserting the beak

into the beak holder, and its eye lid was temporarily pulled back to get an unobstructed view of the eye. Additional local anaesthesia to the cornea was provided using Oxibuprocaine-hydrochloride. Upon locating the sclera-cornea junction at the dorso-temporal side of the eye with a stereoscope (Leica M400E, Wetzlar, Germany), a 27G needle was used to puncture the sclera, avoiding nearby blood capillaries from getting ruptured. This puncture was subsequently used as an entry point for the Hamilton syringe attached to a blunt 33G needle (VWR International GmbH, Germany), carrying the AAV2/9 viral suspension.

To minimize any unintentional damage to the bird's vision, we carefully avoided the lens by using an insertion angle of ~60°–70° relative to the eye's coronal axis (Figure 2). Afterwards, the Hamilton syringe was inserted down to the fundus, and 10–20 μL of viral suspension was injected close to the retinal surface with an approximate speed of ~1 μL/s. The syringe was held in place for at least 10 s after the injection in order to prevent reflux and to ensure dispersion of the viral suspension and carefully retracted afterwards. Post-surgery, the bird was taken out of the injection apparatus and transferred onto a warming plate for quick recovery. Each bird

FIGURE 2
Intravitreal injection route. For intravitreal injections, the lens was bypassed using an insertion angle of ~60–70° relative to the eye's coronal axis to inject the viral suspension (brown) close to the retinal surface (red).
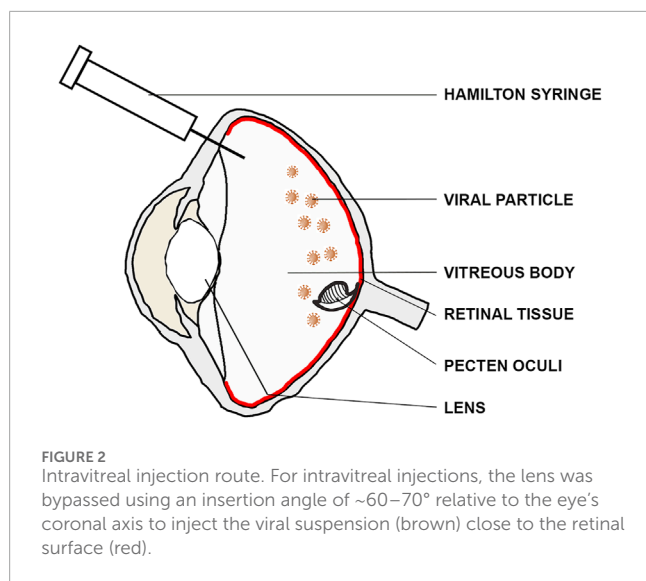
was monitored until it recovered from anesthesia and returned to its home cage upon gaining full consciousness. We provided post-surgical analgesia (Meloxicam administered intramuscularly; 0.2 mL/kg body weight dissolved in 0.9% NaCl) for up to 72 h post-surgery to minimize any signs of discomfort resulting from the surgery. For legal and ethical reasons, we did not perform vehicle-only controls as we had a strictly limited number of wild caught birds available. However, in order to validate the general functionality of the virus, we only injected one eye with the virus, while leaving the contralateral one as a negative control for subsequent immunostainings.

Tissue processing

In line with previous studies on virus-mediated transduction of retinal tissue (Waldner et al., 2019; Nieuwenhuis et al., 2023), we let the AAV2/9 suspension reside inside the injected eye for 21–25 days, following which the birds were sacrificed by decapitation and the injected eye was dissected from the skull. The anterior part of the eye was removed along its coronal axis using a sharp razor blade and the vitreous body was carefully taken out. The eye cup was fixed using 4% paraformaldehyde [PFA dissolved in 0.1 M phosphate buffered saline, pH 7.6 (PBS)] for 30 min. Subsequently, the eye cups were washed three times in PBS for 15 min each and cryoprotected in a graded series of sucrose solutions (10%, 20%, 30% dissolved in 0.1 M PBS) overnight. If necessary, the eyecups were stored in 30% sucrose solution at −20°C until they were subjected to immunohistochemistry.

Immunohistochemistry

Retinal tissue was cryosectioned on a freezing microtome (Leica CM 1860; Wetzlar, Germany) into serial cross sections with a thickness of 30 μm and placed onto microscope slides (epredia, Superfrost Plus Adhesion slides, Fisher Scientific, Waltham, MA, United States). For EGFP immunohistochemistry, the slides were

briefly dried on a warming plate and washed twice with 0.1 M PBS for 15 min. Unspecific binding sites were blocked using 5% donkey serum (Sigma-Aldrich, Burlington, MA, United States) and 0.3%–0.5% Triton X-100 (Carl Roth, Germany) dissolved in 0.1 M PBS for 1–2 h. The slides were subsequently incubated overnight with a goat anti-GFP antibody (diluted 1:500 in blocking solution; 600-101-215; RRID: AB_218182; Rockland, Pottstown, PA, United States) together with one of the opsin antibodies listed in Table 1 at 4°C to assess the type of transduced photoreceptors. On the following day, slides were washed thrice for 10–15 min each in 0.1 M PBS. The retinal slices were subsequently incubated with appropriate secondary antibodies (Alexa Fluor 488-conjugated (anti goat) for EGFP; Alexa 568-conjugated (anti mouse) for rhodopsin; Alexa647-conjugated (anti guinea pig) for red opsin; Alexa 568-conjugated (anti mouse) for green opsin; Alexa 568 (anti rat) for blue opsin; Alexa 568 (anti rabbit) for UV opsin; dilution 1:500, Thermo Fisher Scientific, Waltham, MA, United States) for 2 h. The slices were washed thrice with PBS for 10–15 min and mounted with Vectashield mounting medium (containing nuclear DAPI stain; BIOZOL, Germany).

Image acquisition, processing, and quantification

Retinal sections were imaged with a confocal laser scanning microscope (Leica TCS SP8, Leica Microsystems, Wetzlar, Germany), using a HC PL APO 40x/1.3 or HC PL APO 63x/1.4 oil immersion objective. We used the "Navigator" software (LAS X Life Science, Wetzlar, Germany) to image retinal sections from each transduced eye. Twelve to fourteen retinal sections across the entire eye cup were used to determine the transduction efficiency in each transduced eye. Each section was individually analyzed as follows: 1) We normalized the intensity using the *Contrast Enhancement* tool (0.2%) in Fiji (Schindelin et al., 2012). 2) Both the transduced area and the total retina area on each section were individually marked using the *Freehand* tool. 3) The *Measure* tool was used to obtain the respective area sizes, and the fraction of transduced area was calculated for each individual section. To estimate the transduction efficiency per total retina, we used spline extrapolation to predict the values of the slides interjacent to the analyzed ones. We then averaged all values to calculate the fraction of transduced retina area. Figures 3C, D, G, H display the series of multiple Z-stack images (0.27 μm step size) merged into a maximum projection image. High-resolution scans of EGFP-labeled photoreceptors were normalized in Fiji using the *Contrast Enhancement* function.
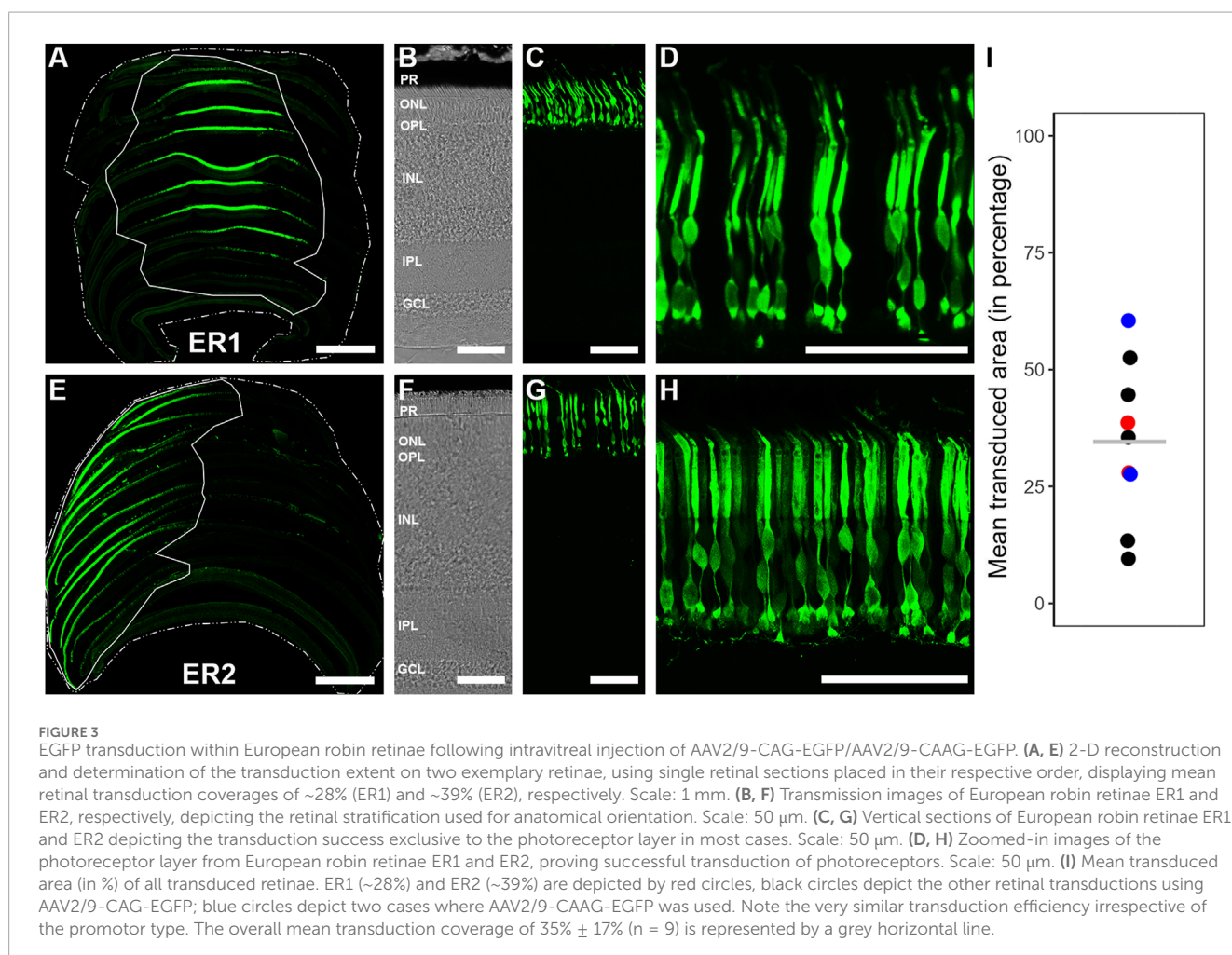
Results

Transduction coverage of european robin retina

Intravitreal ocular injection of AAV2/9 successfully transduced retinal tissue of European robins (Figures 3A–H). The transduced area ranged from 10% to 60% of the total retinal surface (Figure 3I), resulting in an overall mean transduction coverage of ~35 ± 17% across nine individuals, which we considered

TABLE 1 Opsin antibodies used in this study.

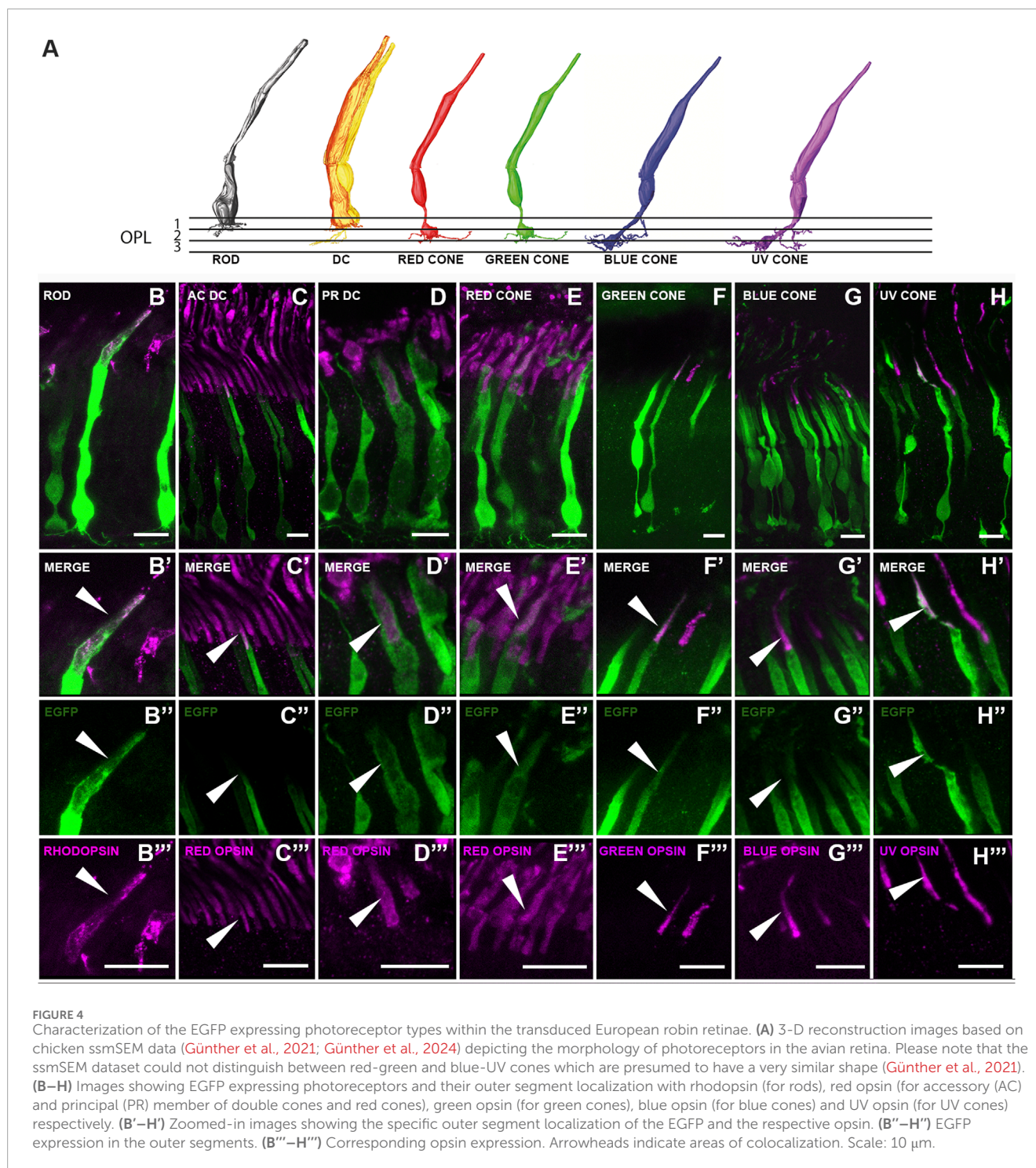| Opsin antibody	Clone/company/catalogue number	Host species	Dilution	Immunogen sequence
Rhodopsin	Clone 1D4/Cell essentials/ab5417	Mouse	1:500	Detailed sequence not provided by the manufacturer
Red opsin	Karl W. Koch lab/Davids Biotechnologies	Guinea pig	1:1,000	SRYWPHGLKTSCGPDVFSGSSDP GVQSYMVSI
Green opsin	OPSG2 clone 26G5/Helmholtz Munich	Mouse	1:500	GPDYYTHNPDFH
Blue opsin[a]	OPSB clone 2D6/Helmholtz Munich	Rat	1:5	MHPPRPTTDLPEDF
UV opsin (Opsin, blue)	Millipore/AB5407	Rabbit	1:500	Recombinant human blue opsin

[a]BLUE opsin (OPSB) (Günther et al., 2018).

FIGURE 3
EGFP transduction within European robin retinae following intravitreal injection of AAV2/9-CAG-EGFP/AAV2/9-CAAG-EGFP. **(A, E)** 2-D reconstruction and determination of the transduction extent on two exemplary retinae, using single retinal sections placed in their respective order, displaying mean retinal transduction coverages of ~28% (ER1) and ~39% (ER2), respectively. Scale: 1 mm. **(B, F)** Transmission images of European robin retinae ER1 and ER2, respectively, depicting the retinal stratification used for anatomical orientation. Scale: 50 μm. **(C, G)** Vertical sections of European robin retinae ER1 and ER2 depicting the transduction success exclusive to the photoreceptor layer in most cases. Scale: 50 μm. **(D, H)** Zoomed-in images of the photoreceptor layer from European robin retinae ER1 and ER2, proving successful transduction of photoreceptors. Scale: 50 μm. **(I)** Mean transduced area (in %) of all transduced retinae. ER1 (~28%) and ER2 (~39%) are depicted by red circles, black circles depict the other retinal transductions using AAV2/9-CAG-EGFP; blue circles depict two cases where AAV2/9-CAAG-EGFP was used. Note the very similar transduction efficiency irrespective of the promotor type. The overall mean transduction coverage of 35% ± 17% (n = 9) is represented by a grey horizontal line.

consistent enough to act as a "proof of principle" for the effectiveness of the viral serotype. We observed heterogenous transduction densities of EGFP expressing neurons, with the highest numbers usually being proximal to the injection site and a gradual decrease with distance. Figures 3A, E display

two exemplary 2-D reconstructions, demonstrating the retinal surface transduction coverage and its regional variability. As expected, in the non-transduced control eyes, no EGFP signal was observed, thereby validating the general functionality of the virus (data not shown).

FIGURE 4
Characterization of the EGFP expressing photoreceptor types within the transduced European robin retinae. **(A)** 3-D reconstruction images based on chicken ssmSEM data (Günther et al., 2021; Günther et al., 2024) depicting the morphology of photoreceptors in the avian retina. Please note that the ssmSEM dataset could not distinguish between red-green and blue-UV cones which are presumed to have a very similar shape (Günther et al., 2021). **(B–H)** Images showing EGFP expressing photoreceptors and their outer segment localization with rhodopsin (for rods), red opsin (for accessory (AC) and principal (PR) member of double cones and red cones), green opsin (for green cones), blue opsin (for blue cones) and UV opsin (for UV cones) respectively. **(B'–H')** Zoomed-in images showing the specific outer segment localization of the EGFP and the respective opsin. **(B''–H'')** EGFP expression in the outer segments. **(B'''–H''')** Corresponding opsin expression. Arrowheads indicate areas of colocalization. Scale: 10 μm.

Types of transduced neurons in the European robin retina

We enhanced the endogenous EGFP signal with an EGFP antibody to identify the type and detailed morphology of the transduced neurons. The vast majority of EGFP reporter gene expression was found in the photoreceptor layer (Figures 3C, D, G, H). Only in very few cases, we observed EGFP expressing Müller cells, potentially resulting from occasional disruption of the inner limiting membrane (ILM) formed by Müller cell endfeet during the viral injections.

To further characterize the photoreceptor types transduced by the ocular injections, immunostainings were carried out using various opsin antibodies (Table 1; Figures 4B–H, B'–H', B''–H'', B'''–H'''). AAV2/9-EGFP targeted all photoreceptor types, i.e., rods, principal and accessory members of double cones, and the four types of single cones (red, green, blue and UV) (Figure 4). Their overall morphology largely resembled the ssmSEM-based

reconstructions of chicken photoreceptors (Günther et al., 2021; Günther et al., 2024) (Figure 4A), thereby validating their morphology in the European robin: rods possessed a stout cell body and terminal with long telodendria; the accessory member of double cones was characterized by a thinner cell body with a distinct brush-like synaptic terminal located far more distal than all other terminals; the principal member of the double cones has a very broad shape and rather thick outer segment; the four single cones (red, green, blue and UV) were observed to have a thin cell body and bulb like terminal endings.

In addition to using a ubiquitous CAG promoter for seven specimens, two additional ocular injections were performed using a CAAG promoter. Both promoters resulted in a very similar high retinal transduction efficiency and variability (see blue dots in Figure 3I), thereby validating the effectiveness of the used serotype irrespective of the promoter.

Discussion

In contrast to both the subretinal (Barker et al., 2009; Watanabe et al., 2013; Petit et al., 2017) and intravitreal route of injection (Giove et al., 2010; Reid et al., 2017), which have proven successful in transducing considerable amounts of retinal tissue in murine model systems, only the intravitreal route, due to its less invasiveness, appears feasible in avian model systems. However, so far, the intravitreal route has not yielded efficient and widespread transduction of retinal tissue in birds (Waldner et al., 2019). This could have been caused by the large relative volume of the vitreous chamber in birds and the much thicker nerve fiber layer in avian eyes, which may act as a barrier for successful transductions. The main reason, however, might have been the lack of appropriate AAV serotypes capable of successfully transducing the retina. In this study, the AAV2/9 serotype proved successful in transducing European robin retinal tissue, reaching widespread transduction coverages of ~35 ± 17% of the total retinal surface (Figure 3I) across seven individuals. Bearing in mind that volumetric calculations indicate that European robin´s eyes are approximately 20 times larger than mouse eyes, increasing the injected volume and/or titer concentration could potentially improve the transduction efficiency even further.

In this "proof of principle" study, transduction efficiency varied between 10% and 60%. Potential reasons for this variability include 1) different amounts of viral suspension, ranging between 10 and 20 µL, 2) occasional efflux of viral suspension during injection, and 3) variable virus titers (ranging between ~2-4 × 10^{12}). Since it is well documented that a certain concentration of viruses is required to induce transduction (Giove et al., 2010; Reid et al., 2017; Waldner et al., 2019), these variations may have impacted the transduction efficiency.

Given the observed variability, future studies investigating functional aspects effects of genetic manipulations using the AAV2/9 serotype as a vehicle will require a more thorough quantitative assessment of transduction efficiency, e.g., by Western blots and/or RT-qPCR.

Avian AAVs (A3Vs) have been used for intravitreal injections in birds, but showed limited transduction efficiency (Waldner et al., 2019). In search for a suitable AAV capable to successfully transduce

retinal tissue of European robins, a thorough literature survey revealed that, in contrast to AAV5 and AAV8, both AAV2 and AAV9 displayed a highly specific tropism towards various retinal cell types in mice (Lee et al., 2018). Pseudotyping, i.e., a recombinant AAV containing the structural and enzymatic component from one AAV "wrapped" in the capsid component from another, can further increase the tropism towards certain host cells. Here, we used AAV2/9-CAG-EGFP and AAV2/9-CAAG-EGFP for intravitreal delivery in the European robin retina. This serotype was chosen as it can transfect a broad range of retinal cell types, including photoreceptors and its progenitors (Allocca et al., 2007) in other vertebrate species (Watanabe et al., 2013).

We can only speculate on why AAV2/9 outperformed A3Vs in intravitreal injections in the avian retina. The vitreoretinal junction (inner limiting membrane, ILM) is a serotype specific barrier for naturally occurring AAVs in mice (Dalkara et al., 2009). It contains AAV binding sites, which create a diffusion barrier for AAV particles that arrive from the intravitreal side (Khabou et al., 2016). Thus, one potential explanation could be that the avian ILM contains more binding sites for avian AAVs (A3V) than for non-avian AAV2/9 particles, leading to the larger transduction efficiency of AAV2/9 in the avian retina. However, differences in virus titer, injection routine, or study species may also play a role.

Demonstrating the connectivity between photoreceptors and bipolar cells (Günther et al., 2021; Balaji et al., 2023; Günther et al., 2024) or horizontal cells (Günther et al., 2025) and successfully enabling photoreceptor-specific gene delivery to the European robin retina, might only be the first of many steps towards a plethora of investigations on the morphology, biochemistry and physiology of the avian retina using the AAV2/9 serotype. This is of particular importance, since birds, as mentioned before, have some of the most high-performing eyes amongst vertebrates, but so far, we have lacked the necessary tools to genetically manipulate them. Its proven functionality in European robins makes AAV 2/9 particularly well suited for studying the proposed light dependent, radical pair based magnetoreception mechanism (Hore and Mouritsen, 2016; Mouritsen, 2018; Mouritsen, 2022). This elusive sense (Zapka et al., 2009; Hore and Mouritsen, 2016; Wu et al., 2020; Wang et al., 2021; Xu et al., 2021; Görtemaker et al., 2022) is likely to be based on magnetically sensitive reactions inside the cryptochrome 4 protein (Xu et al., 2021; Chetverikova et al., 2022) located in the outer segments of double cones and long wavelength single cones (Günther et al., 2018). We are convinced that the AAV 2/9 serotype, which we identified here, will be instrumental to explore the physiology of European robin photoreceptors and the role of double cones in magnetoreception.

Data availability statement

The datasets presented in this study can be found in online repositories. The names of the repository/repositories and accession number(s) can be found below: https://www.addgene.org/29778/, Addgene plasmid #29778. The original dataset of this study will be made available from the corresponding author upon request, without undue reservation. Anti-Green opsin antibody can be

obtained from Monoclonal Antibody Core Facility at Helmholtz Center Munich.

Ethics statement

Author contributions

PS: Conceptualization, Data curation, Formal Analysis, Investigation, Methodology, Validation, Visualization, Writing–original draft, Writing–review and editing. DH: Conceptualization, Data curation, Formal Analysis, Funding acquisition, Investigation, Methodology, Supervision, Validation, Visualization, Writing–original draft, Writing–review and editing. BS: Formal Analysis, Investigation, Methodology, Visualization, Writing–original draft, Writing–review and editing. EM: Methodology, Resources, Writing–review and editing. KH: Methodology, Writing–review and editing. LB: Methodology, Writing–review and editing. IM: Methodology, Writing–review and editing. K-WK: Funding acquisition, Methodology, Resources, Writing–review and editing. RF: Methodology, Resources, Writing–review and editing. CS: Methodology, Resources, Writing–review and editing. KD: Conceptualization, Funding acquisition, Methodology, Supervision, Writing–review and editing. HM: Conceptualization, Funding acquisition, Supervision, Writing–review and editing.

Funding

Acknowledgments

Conflict of interest

The authors declare that the research was conducted in the absence of any commercial or financial relationships that could be construed as a potential conflict of interest.

The author(s) declared that they were an editorial board member of Frontiers, at the time of submission. This had no impact on the peer review process and the final decision.

Generative AI statement

The author(s) declare that no Generative AI was used in the creation of this manuscript.

Publisher's note

All claims expressed in this article are solely those of the authors and do not necessarily represent those of their affiliated organizations, or those of the publisher, the editors and the reviewers. Any product that may be evaluated in this article, or claim that may be made by its manufacturer, is not guaranteed or endorsed by the publisher.

References

Ahmadiantehrani, S., and London, S. E. (2017). A reliable and flexible gene manipulation strategy in posthatch zebra finch brain. *Sci. Rep.* 7 (1), 43244. doi:10.1038/srep43244

Ali, R. R., Sarra, G. M., Stephens, C., Alwis, M. D., Bainbridge, J. W., Munro, P. M., et al. (2000). Restoration of photoreceptor ultrastructure and function in retinal degeneration slow mice by gene therapy. *Nat. Genet.* 25 (3), 306–310. doi:10.1038/77068

Allocca, M., Mussolino, C., Garcia-Hoyos, M., Sanges, D., Iodice, C., Petrillo, M., et al. (2007). Novel adeno-associated virus serotypes efficiently transduce murine photoreceptors. *J. Virol.* 81 (20), 11372–11380. doi:10.1128/jvi.01327-07

Atchison, R. W., Casto, B. C., and Hammon, W. M. (1965). Adenovirus-associated defective virus particles. *Science* 149 (3685), 754–756. doi:10.1126/science.149.3685.754

Bacci, G. M., Becherucci, V., Marziali, E., Sodi, A., Bambi, F., and Caputo, R. (2022). Treatment of inherited retinal dystrophies with somatic cell therapy medicinal product: a review. *Life* 12 (5), 708. doi:10.3390/life12050708

Balaji, V., Haverkamp, S., Seth, P. K., Günther, A., Mendoza, E., Schmidt, J., et al. (2023). Immunohistochemical characterization of bipolar cells in four distantly related avian species. *J. Comp. Neurology* 531 (4), 561–581. doi:10.1002/cne.25443

Balakrishnan, B., and Jayandharan, R. (2014). Basic biology of adeno-associated virus (AAV) vectors used in gene therapy. *Curr. Gene. Ther.* 14 (2), 86–100. doi:10.2174/1566523214666140302193709

Barker, S. E., Broderick, C. A., Robbie, S. J., Duran, Y., Natkunarajah, M., Buch, P., et al. (2009). Subretinal delivery of adeno-associated virus serotype 2 results in minimal immune responses that allow repeat vector administration in immunocompetent mice. *J. Gene. Med.* 11 (6), 486–497. doi:10.1002/jgm.1327

Bennett, J., Wilson, J., Sun, D., Forbes, B., and Maguire, A. (1994). Adenovirus vector-mediated *in vivo* gene transfer into adult murine retina. *Investigative Ophthalmol. and Vis. Sci.* 35 (5), 2535–2542.

Buch, P. K., Bainbridge, J. W., and Ali, R. R. (2008). AAV-mediated gene therapy for retinal disorders: from mouse to man. *Gene. Ther.* 15 (11), 849–857. doi:10.1038/gt.2008.66

Burton, R. F. (2008). The scaling of eye size in adult birds: relationship to brain, head and body sizes. *Vis. Res.* 48 (22), 2345–2351. doi:10.1016/j.visres.2008.08.001

Cebulla, C. M., Zelinka, C. P., Scott, M. A., Lubow, M., Bingham, A., Rasiah, S., et al. (2012). A chick model of retinal detachment: cone rich and novel. *PLoS. One.* 7 (9), e44257. doi:10.1371/journal.pone.0044257

Chetverikova, R., Dautaj, G., Schwigon, L., Dedek, K., and Mouritsen, H. (2022). Double cones in the avian retina form an oriented mosaic which might facilitate magnetoreception and/or polarized light sensing. *J. R. Soc. Interface* 19 (189), 20210877. doi:10.1098/rsif.2021.0877

Dalkara, D., Kolstad, K. D., Caporale, N., Visel, M., Klimczak, R. R., Schaffer, D. V., et al. (2009). Inner limiting membrane barriers to AAV-mediated retinal transduction from the vitreous. *Mol. Ther.* 17(12):2096–2102. doi:10.1038/mt.2009.181

Giove, T. J., Sena-Esteves, M., and Eldred, W. D. (2010). Transduction of the inner mouse retina using AAVrh8 and AAVrh10 via intravitreal injection. *Exp. Eye Res.* 91 (5), 652–659. doi:10.1016/j.exer.2010.08.011

Görtemaker, K., Yee, C., Bartölke, R., Behrmann, H., Voß, J. O., Schmidt, J., et al. (2022). Direct interaction of avian cryptochrome 4 with a cone specific G-protein. *Cells* 11 (13), 2043. doi:10.3390/cells11132043

Günther, A., Balaji, V., Leberecht, B., Forst, J. J., Rotov, A. Y., Woldt, T., et al. (2025). Morphology and connectivity of retinal horizontal cells in two avian species. *Front. Cell. Neurosci.* 19. doi:10.3389/fncel.2025.1558605

Günther, A., Dedek, K., Haverkamp, S., Irsen, S., Briggman, K. L., and Mouritsen, H. (2021). Double cones and the diverse connectivity of photoreceptors and bipolar cells in an avian retina. *J. Neurosci.* 41 (23), 5015–5028. doi:10.1523/JNEUROSCI.2495-20.2021

Günther, A., Einwich, A., Sjulstok, E., Feederle, R., Bolte, P., Koch, K. W., et al. (2018). Double-cone localization and seasonal expression pattern suggest a role in magnetoreception for European robin cryptochrome 4. *Curr. Biol.* 28 (2), 211–223. doi:10.1016/j.cub.2017.12.003

Günther, A., Haverkamp, S., Irsen, S., Watkins, P. V., Dedek, K., Mouritsen, H., et al. (2024). Species–specific circuitry of double cone photoreceptors in two avian retinas. *Commun. Biol.* 7 (1), 992. doi:10.1038/s42003-024-06697-2

Güntürkün, O., Miceli, D., and Watanabe, M. (1993). *Anatomy of the avian thalamofugal pathway*. Cambridge: MIT Press.

Harpavat, S., and Cepko, C. L. (2006). RCAS-RNAi: a loss-of-function method for the developing chick retina. *Bmc. Dev. Biol.* 6, 2–7. doi:10.1186/1471-213X-6-2

Haverkamp, S., Albert, L., Balaji, V., Němec, P., and Dedek, K. (2021). Expression of cell markers and transcription factors in the avian retina compared with that in the marmoset retina. *J. Comp. Neurol.* 529 (12), 3171–3193. doi:10.1002/cne.25154

Hore, P. J., and Mouritsen, H. (2016). The radical-pair mechanism of magnetoreception. *Annu. Rev. Biophys.* 45 (1), 299–344. doi:10.1146/annurev-biophys-032116-094545

Isiegas, C., Marinich-Madzarevich, J. A., Marchena, M., Ruiz, J. M., Cano, M. J., de la Villa, P., et al. (2016). Intravitreal injection of proinsulin-loaded microspheres delays photoreceptor cell death and vision loss in the rd10 mouse model of retinitis pigmentosa. *Invest. Ophthalmol. Vis. Sci.* 57 (8), 3610–3618. doi:10.1167/iovs.16-19300

Jeon, C. J., Strettoi, E., and Masland, R. H. (1998). The major cell populations of the mouse retina. *J. Neurosci.* 18 (21), 8936–8946. doi:10.1523/JNEUROSCI.18-21-08936.1998

Jomary, C., Piper, T. A., Dickson, G., Couture, L. A., Smith, A. E., Neal, M. J., et al. (1994). Adenovirus-mediated gene transfer to murine retinal cells *in vitro* and *in vivo*. *Febs. Lett.* 347 (2-3), 117–122. doi:10.1016/0014-5793(94)00512-5

Jones, M. P., Pierce Jr, K. E., and Ward, D. (2007). Avian vision: a review of form and function with special consideration to birds of prey. *J. Exot. Pet. Med.* 16 (2), 69–87. doi:10.1053/j.jepm.2007.03.012

Kansara, V., Muya, L., Wan, C. R., and Ciulla, T. A. (2020). Suprachoroidal delivery of viral and nonviral gene therapy for retinal diseases. *J. Ocul. Pharmacol. Ther.* 36 (6), 384–392. doi:10.1089/jop.2019.0126

Khabou, H., Desrosiers, M., Winckle, C., Fouquet, S., Auregan, G., Bemelmans, A.-P., et al. (2016). Insight into the mechanisms of enhanced retinal transduction by the engineered AAV2 capsid variant -7m8. *Biotechnol. Bioeng.* 113(12):2712–2724. doi:10.1002/bit.26031

Lee, S. H., Yang, J. Y., Madrakhimov, S., Park, H. Y., Park, K., and Park, T. K. (2018). Adeno-associated viral vector 2 and 9 transduction is enhanced in streptozotocin-induced diabetic mouse retina. *Mol. Ther. Methods Clin. Dev.* 13, 55–66. doi:10.1016/j.omtm.2018.11.008

Li, T., Adamian, M., Roof, D. J., Berson, E. L., Dryja, T. P., Roessler, B. J., et al. (1994). *In vivo* transfer of a reporter gene to the retina mediated by an adenoviral vector. *Invest. Ophthalmol. Vis. Sci.* 35 (5), 2543–2549.

Mouritsen, H. (2018). Long-distance navigation and magnetoreception in migratory animals. *Nature* 558 (7708), 50–59. doi:10.1038/s41586-018-0176-1

Mouritsen, H. (2022). "Magnetoreception in birds and its use for long-distance migration," in *Sturkie's avian physiology* (Academic Press), 233–256. doi:10.1016/B978-0-12-819770-7.00040-2

Mühlfriedel, R., Michalakis, S., Garrido, M. G., Biel, M., and Seeliger, M. W. (2013). Optimized technique for subretinal injections in mice. *Methods. Mol. Biol.* 935, 343–349. doi:10.1007/978-1-62703-080-9_24

Nieuwenhuis, B., Laperrousaz, E., Tribble, J. R., Verhaagen, J., Fawcett, J. W., Martin, K. R., et al. (2023). Improving adeno-associated viral (AAV) vector-mediated transgene expression in retinal ganglion cells: comparison of five promoters. *Gene Ther.* 30(6):503–519. doi:10.1038/s41434-022-00380-z

Niu, X., Jiang, Z., Peng, Y., Huang, S., Wang, Z., and Shi, L. (2022). Visual cognition of birds and its underlying neural mechanism: a review. *Avian. Res.* 13, 100023. doi:10.1016/j.avrs.2022.100023

Ong, T., Pennesi, M. E., Birch, D. G., Lam, B. L., and Tsang, S. H. (2019). Adeno-associated viral gene therapy for inherited retinal disease. *Pharm. Res.* 36 (2), 34. doi:10.1007/s11095-018-2564-5

Park, S. W., Kim, J. H., Park, W. J., and Kim, J. H. (2015). Limbal approach-subretinal injection of viral vectors for gene therapy in mice retinal pigment epithelium. *J. Vis. Exp.* 102, 53030. doi:10.3791/53030

Petit, L., Ma, S., Cheng, S. Y., Gao, G., and Punzo, C. (2017). Rod outer segment development influences AAV-mediated photoreceptor transduction after subretinal injection. *Hum. Gene. Ther.* 28 (6), 464–481. doi:10.1089/hum.2017.020

Reid, C. A., Ertel, K. J., and Lipinski, D. M. (2017). Improvement of photoreceptor targeting via intravitreal delivery in mouse and human retina using combinatory rAAV2 capsid mutant vectors. *Invest. Ophthalmol. Vis. Sci.* 58 (14), 6429–6439. doi:10.1167/iovs.17-22281

Ronzitti, G., Gross, D. A., and Mingozzi, F. (2020). Human immune responses to adeno-associated virus (AAV) vectors. *Front. Immunol.* 11, 670. doi:10.3389/fimmu.2020.00670

Rotov, A. Y., Goriachenkov, A. A., Cherbunin, R. V., Firsov, M. L., Chernetsov, N., and Astakhova, L. A. (2022). Magnetoreceptory function of European robin retina: electrophysiological and morphological non-homogeneity. *Cells.* 11(19):3056. doi:10.3390/cells11193056

Schindelin, J., Arganda-Carreras, I., Frise, E., Kaynig, V., Longair, M., Pietzsch, T., et al. (2012). Fiji: an open-source platform for biological-image analysis. *Nat. Methods.* 9 (7), 676–682. doi:10.1038/nmeth.2019

Schlichtenbrede, F. C., MacNeil, A., Bainbridge, J. W. B., Tschernutter, M., Thrasher, A. J., Smith, A. J., et al. (2003). Intraocular gene delivery of ciliary neurotrophic factor results in significant loss of retinal function in normal mice and in the Prph2Rd2/Rd2 model of retinal degeneration. *Gene. Ther.* 10 (6), 523–527. doi:10.1038/sj.gt.3301929

Scott, B. B., and Lois, C. (2005). Generation of tissue-specific transgenic birds with lentiviral vectors. *Proc. Natl. Acad. Sci. USA.* 102 (45), 16443–16447. doi:10.1073/pnas.0508437102

Seifert, M., Baden, T., and Osorio, D. (2020). The retinal basis of vision in chicken. *Semin. Cell Dev. Biol.* 106, 106–115. doi:10.1016/j.semcdb.2020.03.011

Stieger, K., Cronin, T., Bennett, J., and Rolling, F. (2011). Adeno-associated virus mediated gene therapy for retinal degenerative diseases. *Methods. Mol. Biol.* 807, 179–218. doi:10.1007/978-1-61779-370-7_8

Vergara, M. N., and Canto-Soler, M. V. (2012). Rediscovering the chick embryo as a model to study retinal development. *Neural. Dev.* 7, 22–19. doi:10.1186/1749-8104-7-22

Verrier, J. D., Madorsky, I., Coggin, W. E., Geesey, M., Hochman, M., Walling, E., et al. (2011). Bicistronic lentiviruses containing a viral 2A cleavage sequence reliably co-express two proteins and restore vision to an animal model of LCA1. *PloS. One.* 6 (5), e20553. doi:10.1371/journal.pone.0020553

Waldner, D. M., Visser, F., Fischer, A. J., Bech-Hansen, N. T., and Stell, W. K. (2019). Avian adeno-associated viral transduction of the postembryonic chicken retina. *Transl. Vis. Sci. Technol.* 8(4), 1–1. doi:10.1167/tvst.8.4.1

Waldvogel, J. A. (1990). The bird's eye view. *Am. Sci.* 78 (4), 342–353.

Wang, X., Jiang, B., Gu, L., Chen, Y., Mora, M., Zhu, M., et al. (2021). A photoregulatory mechanism of the circadian clock in Arabidopsis. *Nat. Plants* 7 (10), 1397–1408. doi:10.1038/s41477-021-01002-z

Watanabe, S., Sanuki, R., Ueno, S., Koyasu, T., Hasegawa, T., and Furukawa, T. (2013). Tropisms of AAV for subretinal delivery to the neonatal mouse retina and its application for *in vivo* rescue of developmental photoreceptor disorders. *PloS. One.* 8 (1), e54146. doi:10.1371/journal.pone.0054146

Williams, M. L., Coleman, J. E., Haire, S. E., Aleman, T. S., Cideciyan, A. V., Sokal, I., et al. (2006). Lentiviral expression of retinal guanylate cyclase-1 (RetGC1) restores vision in an avian model of childhood blindness. *PLoS Med.* 3 (6), e201. doi:10.1371/journal.pmed.0030201

Wiltschko, W., Munro, U., Ford, H., and Wiltschko, R. (1993). Red light disrupts magnetic orientation of migratory birds. *Nature* 364, 525–527. doi:10.1038/364525a0

Wu, H., Scholten, A., Einwich, A., Mouritsen, H., and Koch, K. W. (2020). Protein-protein interaction of the putative magnetoreceptor cryptochrome 4 expressed in the avian retina. *Sci. Rep.* 10 (1), 7364. doi:10.1038/s41598-020-64429-y

Xu, J., Jarocha, L. E., Zollitsch, T., Konowalczyk, M., Henbest, K. B., Richert, S., et al. (2021). Magnetic sensitivity of cryptochrome 4 from a migratory songbird. *Nature* 594 (7864), 535–540. doi:10.1038/s41586-021-03618-9

Yiu, G., Chung, S. H., Mollhoff, I. N., Nguyen, U. T., Thomasy, S. M., Yoo, J., et al. (2020). Suprachoroidal and subretinal injections of AAV using transscleral microneedles for retinal gene delivery in nonhuman primates. *Mol. Ther. Methods. Clin. Dev.* 16, 179–191. doi:10.1016/j.omtm.2020.01.002

Zapka, M., Heyers, D., Hein, C. M., Engels, S., Schneider, N.-L., Hans, J., et al. (2009). Visual but not trigeminal mediation of magnetic compass information in a migratory bird. *Nature* 461 (7268), 1274–1277. doi:10.1038/nature08528

Ziccardi, L., Cordeddu, V., Gaddini, L., Matteucci, A., Parravano, M., Malchiodi-Albedi, F., et al. (2019). Gene therapy in retinal dystrophies. *Int. J. Mol. Sci.* 20 (22), 5722. doi:10.3390/ijms20225722